Quantum Circuit Ansatz Structures for Ising Model & A Comparative Analysis of Classical and Quantum Optimization Methods

Duc Truyen Le*
Department of Physics,
National Tsing Hua University,
Hsinchu, Taiwan 300044, R.O.C.

Vu-Linh Nguyen
Department of Theoretical Physics, University of Science,
Vietnam National University, Ho Chi Minh City 70000, Vietnam

Minh Triet Ha
Rhodes College, Memphis, TN 38112, USA

Cong Ha Nguyen
Département de Physique de l'École normale supérieure, ENS-PSL

Quoc Hung Nguyen
Nano and Energy Center, VNU University of Science,
Vietnam National University, Hanoi, Vietnam

Van-Duy Nguyen†
Phenikaa Institute for Advanced Study,
Phenikaa University, Hanoi 12116, Vietnam
(Dated: November 6, 2024)

Abstract: In this study, we delved into several optimization methods, both classical and quantum, and analyzed the quantum advantage that each of these methods offered, and then we proposed a new combinatorial optimization scheme, deemed as QNSPSA_PSR which combines calculating approximately Fubini-study metric (QNSPSA) and the exact evaluation of gradient by Parameter-Shift Rule (PSR). The QNSPSA_PSR method integrates the QNSPSA computational efficiency with the precise gradient computation of the PSR, improving both stability and convergence speed while maintaining low computational consumption. Our results provide a new potential quantum supremacy in the VQE's optimization subroutine and enhance viable paths toward efficient quantum simulations on Noisy Intermediate Scale Quantum Computing (NISQ) devices. Additionally, we also conducted a detailed study of quantum circuit ansatz structures in order to find the one that would work best with the Ising model and NISQ, which we utilized the symmetry of the investigated model.

Keyword: Ising Model, Variational Quantum Eigensolver, Quantum Optimization, Ansazt Construction

I. INTRODUCTION

Duy bo sung ve QC. From the early stage of studying quantum computer, that by its very quantum nature is promising for a new brightly age of computation coming along with three crucial keys of quantum theory: quantum probabilistics, superposition and entanglement. The distinct properties of quantum computer (QC) from classical computer make it be more unique in application, not only be a upgrade computational speed version of traditional computer. Currently, when the quantum hardware is rather limited on operational stats and noise resilience, despite of the ambiguity of realization of such advantages, Variational Quantum Algorithms (VQAs) are thought to be the best at outperforming conventional computers, which are able to implement well on near-term quantum devices known as the so-called Noisy Intermediate-Scale Quantum (NISQ) computers.

Nowadays, when the quantum revolution is being on the track, big tech companies like IBM, Google, D-Wave, etc. compete to build their own quantum computers to yield the quantum supremacy where the first-ever experimental demonstration achieved by the Google AI Quantum team [1], but that is still far from what we expect the quantum computer could do, while coherence time, connectivity of qubit and qubit number limitations keep us from being able to successfully run a long depth circuit and produce a significant result on the present noisy device, in addition to quantum gate implement issues. Those restrictions would yet be challenging to hardware scientists in the near future, posing obstacles that computer scientists would need to weigh against trainability, precision, and efficiency, nevertheless, these NISQ devices are capable of exploitation. Standing out among quantum algorithms envisioned to beat classical computer which are mostly designed for the fault-tolerant quan-

* leductruyenphys@gapp.nthu.edu.tw
† duy.nguyenvan@phenikaa-uni.edu.vn

tum computer, VQAs turn up regarding as an appropriate candidate compatible with the current defective quantum device to address these constraints. The first two prominent applications of VQAs come up are Variation Quantum Eigensolver (VQE) and Quantum Approximate Optimization Algorithm (QAOA). These inherit the core scheme of a VQA, which is to utilize the hybrid routine, leverage the versatility and computational power of classical computer to handle the computation processing, and use quantum devices to execute the quantum circuit. Hence, in this paper's scope, we will travel through the standard procedures and investigate the properties of different methods implemented in a VQE application.

The structure of this paper is as follows, in Chapter 1, we provide an overview of the Variational Quantum Eigensolver (VQE) procedures. A brief introduction to the Transverse Ising Model and its symmetries is discussed in Chapter 2, which will be utilized to inform the ansatz structure. Subsequently, Chapter 3 delves into optimization methods, encompassing both classical and quantum approaches, where we will propose a new quantum optimization method. The numerical study and experiment are conducted in Chapter 4, and then we make the final conclusion in Chapter 5.

II. VARIATIONAL QUANTUM EIGENSOLVER (VQE)

Them reference cac huong ve VQE VQE was initially proposed by Peruzzo et al. [2, 3] as an efficiently alternative way to compute the ground state energy of a quantum chemistry problem i.e. ground-state He-H$^+$ molecular energy rather than Quantum Phase Estimation (QPE) demanding impractically huge numbers of quantum gates, consequentially, VQE becomes a viable strategy highly well flexible with currently potential quantum resources, that can outpace conventional computers. Following the success of running on the photonic quantum processor combined with the traditional devices, many research works are favored to develop various types of VQA reviewed in Ref. [4, 5]. In essence, what makes VQE (generally VQAs) engrossing that is the trial state analysis step to choosing an ansatz adaptive to particular quantum device architecture and/or problems, subsequently, the suitable ansatz is executed congruently on the NISQ device, the remainders are then handled by the classical computer to generate remarkable results with the aid of error mitigation techniques. Instead of diagonalizing a matrix representation of Hamiltonian $\hat{H}$ to find out eigenvalues, that exponentially scale up the matrix size and calculation overhead in traditional computing as the problem grows up larger, VQE just focus on catching up the ground state energy E_g basically based on the variational principle

$$E_g \leq E\left[\Psi(\boldsymbol{\theta})\right] = \frac{\langle \Psi(\boldsymbol{\theta})|\hat{H}|\Psi(\boldsymbol{\theta})\rangle}{\langle \Psi(\boldsymbol{\theta})|\Psi(\boldsymbol{\theta})\rangle} = \langle \hat{H} \rangle_{\hat{U}(\boldsymbol{\theta})}. \quad (1)$$

The arbitrary quantum state $|\Psi(\boldsymbol{\theta})\rangle \equiv \hat{U}(\boldsymbol{\theta})|\Psi_0\rangle$ is a trial solution, the so-called *ansatz* parametrized by a unitary operator $\hat{U}(\boldsymbol{\theta})$, so that when the parameter $\boldsymbol{\theta}$ varies, the ansatz $|\Psi(\boldsymbol{\theta})\rangle$ is readily capable to span on the relevant quantum space where the ground state located. By modifying $\boldsymbol{\theta}$ value systematically, the VQE task is to travel around spanned space to extract the ground state minimizing the energy function $E\left[\Psi(\boldsymbol{\theta})\right]$ or in general VQA, the energy function described by $\mathcal{L}\left(\boldsymbol{\theta}, \langle \hat{H} \rangle_{\hat{U}(\boldsymbol{\theta})}\right)$, and the objective is

$$\min_{\boldsymbol{\theta}} \mathcal{L}\left(\boldsymbol{\theta}, \langle \hat{H} \rangle_{\hat{U}(\boldsymbol{\theta})}\right). \quad (2)$$

In fact, when the accuracy is not strictly rigorous, the minimum of the energy function is not necessarily required an exactly ground state solution, due to the error in energy being in the second order of the quantum state error. Formally, the classical approach for VQE insists on an analytical expression of the lost function $\mathcal{L}\left(\boldsymbol{\theta}, \langle \hat{H} \rangle_{\hat{U}(\boldsymbol{\theta})}\right)$, in particularly, wave function expression $|\Psi(\boldsymbol{\theta})\rangle$ that becomes eventually unachievable going along with more and more problem complexities. Nevertheless, this weakness is literally the quantum advantage we have in VQE quantum computing approach, quantum computers are adopted to simulate quantum states, and state expectation outcomes are subsequently measured to pipeline to calculate the lost function classically. And partly because of lost function precision greater quadratically than the state function, indeed, we need two states to sandwich operators, VQEs are hereby friendly with noisy devices, which can work out meaningful results even though the states are disturbed by noises. These motivations are robust enough to let us dive deeper into VQE operation, ideally noise-free assumption in this paper's scope though, the noisy one will be addressed in the future study.

The structure of a VQE algorithm is depicted schematically as Fig. 1 within four-basic steps: *Hamiltonian construction, Ansatz preparation, Measurement strategy* and *Optimization.*

Hamiltonian construction: Starting from a given abstract problem, eg. molecule ground state energy, shortest path, transshipment problems, an initially mathematical form called the Hamiltonian $\hat{H}$ is modeled. A mapping scheme is needed to convert $\hat{H}$ into a new form made out of operators that are able to execute on a quantum computer. Invoking prior knowledge of the physical system, particular symmetries are drawn on to simplify the Hamiltonian, such information is usefully reused to guide the erection of other VQE subroutines.

Ansatz preparation: To pick out a good ansatz, an essential condition must be satisfied is that the space spanned by the ansatz contains the desired state extremize objective function. An obvious one is a generic ansatz spread over all Hilbert space, a quantum circuit for that kind of ansatz is usually generated by multi-control-$U_3(\boldsymbol{\theta})$ gates, so that all problems could be ultimately settled without ansatz concern. Nevertheless,
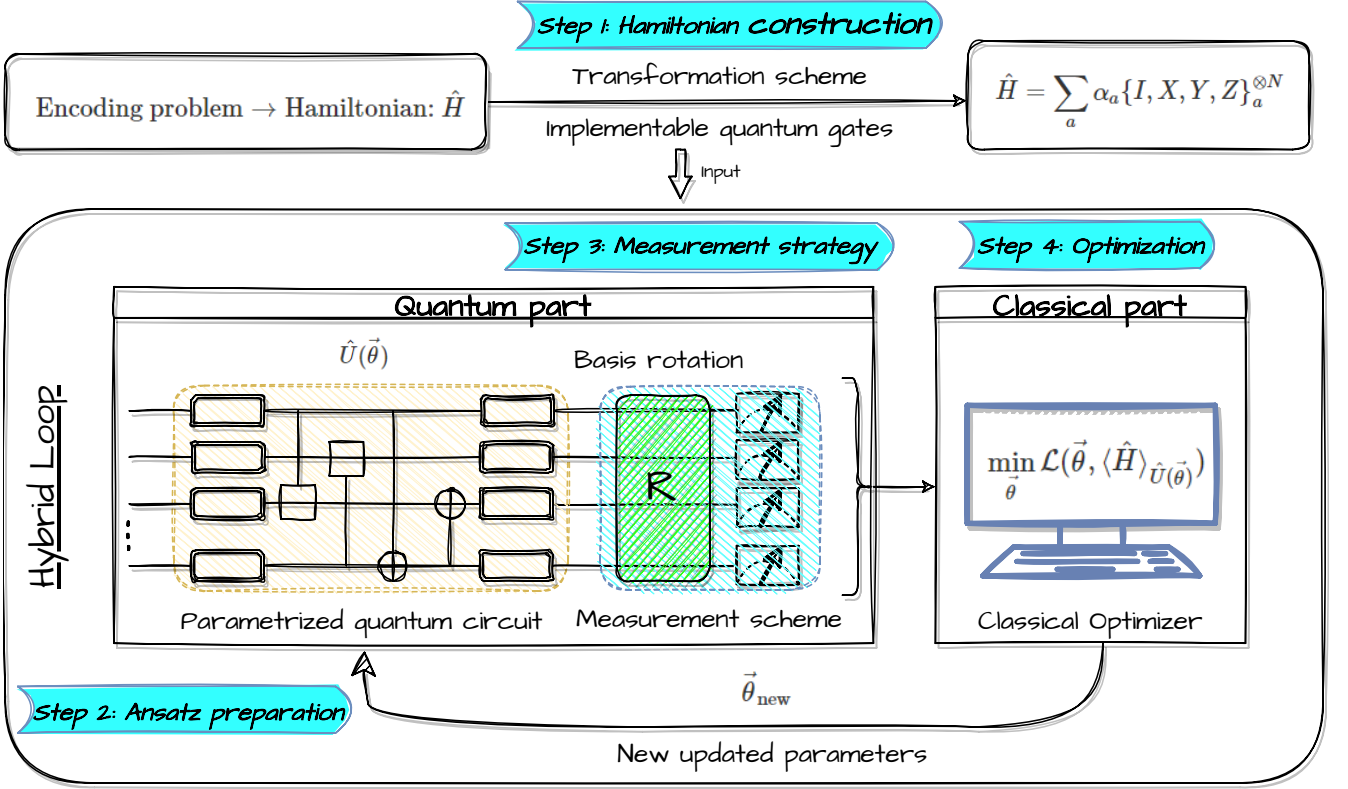
FIG. 1: VQE Architecture

that is not the end of the story, the computation cost of such a multi-control-$U_3(\boldsymbol{\theta})$ gate is extremely high and even unfeasible when deploy on NISQ device. As a consequence, an initial crucial step in VQE is to find an ansatz that is expressive enough to capture the important features of the wavefunction, but also efficient enough to be optimized using optimization techniques. In this article, we employ the approach that excavates up symmetries and physical properties of the physical system to guide the design of the ansatz respecting those symmetries, which helps us considerably reduce the number of training parameters and circuit depth needed in a theoretically speculative way, thereby improves the efficiency of the optimization. There are also other methods, that use a hierarchical ansatz, where the circuit is divided into layers and each layer is optimized independently, and also use machine learning to automatically generate the quantum circuit [6, 7].

Measurement: To reading off information from the wave function to estimate the expectation value of the Hamiltonian, apart from the standard basis measurement where each qubit in the output state is measured in the computational basis, the measurement scheme is manifestly came up with is a unitary transformation to the diagonal basis of observable operators in Hamiltonian, typically is defined by tensor products of Pauli operators, such as X, Y, and Z. Almost Hamiltonian of interest are hermitian and be able to decompose in terms of Pauli strings

$$\hat{H} = \sum_i \otimes_{j=1}^N \sigma_j^i, \qquad (3)$$
$$\sigma_j^i \in \{I, X, Y, Z\},$$

each Pauli string term $P^i = \otimes_{j=1}^N \sigma_j^i$ has likely overlapped the others in somewhere qubit sites, which means $\sigma_j^m \equiv \sigma_j^k$ being able to measure simultaneously, the grouping methods skillfully make use of this information to lower the number of measurements, the symmetry structures of problem are able to exploit as well, and other efficient measurement methods are reviewed in [8]. Those on-research topics are highly crucial to the current NISQ device when a minimum measurement performance is required upon a given restricted number of shots. Furthermore, for a given ϵ accuracy, VQE demands a trade-off $\mathcal{O}(\frac{1}{\epsilon^2})$ number of circuit samples with $\mathcal{O}(1)$ circuit depth compared to other finding ground state energy method, QPE, which consumes $\mathcal{O}(1)$ circuit measurement repetitions with depth $\mathcal{O}(\frac{1}{\epsilon})$. A better approach is essentially proposed to reconcile disadvantages between the two above methods, which is deemed a generalized VQE algorithm, α-VQE, when outrunning VQE by just $\mathcal{O}(\frac{1}{\epsilon^{2(1-\alpha)}})$ circuit samples and lower circuit depth $\mathcal{O}(\frac{1}{\epsilon^\alpha})$ than QPE, where $\alpha \in [0,1]$ [9].

Optimization: Last but not least piece in VQE subroutine is to vary the parameter $\boldsymbol{\theta}$ to catch up the global extreme point (but in many cases, the local one is preferred) in the function of interest described by Eq. (2).

The criteria should be pondered to problem-friendly implement, which are able low-cost function evaluation, fast convergence with a given quantum resources, and silence to noise. Based on different kinds of utilizing objective function information, people classify it into two main optimization approaches: gradient-based, derivative-free. Meanwhile, the gradient-based employs the gradient information in mostly first order, and second order to travel along the steepest direction of the cost function landscape. The derivative-free rather directly uses responses of the objective function at different points in the parameter space to iteratively improve the parameter values, and as usual, these utilize the subroutine classical algorithm and just consume a limited quantum evaluation expense than gradient-based, these are thus seemingly more congruous with NISQ. In the context of VQAs, gradient-free approaches can be used to optimize quantum circuit parameters when computing the gradient is either impractical or excessively costly, for example, when simulating the behavior of a quantum system becomes computationally expensive, or when the objective function cannot be expressed analytically. Nevertheless, the Gradient-based methods are arguably more reliable and have faster convergence as the more complicated structure of the objective function, henceforth, the total trade-off would be shoulder-by-shoulder when deliberately adopting between these two. Furthermore, the step size problem in gradient-based and applying machine learning in derivative-free are active topics research at the stage, see [5] section II.D for more reviews. In the context of this paper, we investigated several optimization methods and instead labelize again those into two regimes, classical and quantum optimization.

III. ANSATZ FOR TRANSVERSE ISING MODEL

A. Transverse Ising model (TIM)

The Transverse Ising model was introduced first in 1963 by de Gennes when he built a model for describing the low-frequency collective modes of protons in the ferroelectric phase of ferroelectric crystals KH_2PO_4 (COLLECTIVE MOTIONS OF HYDROGEN BONDS - de Gennes). From then until now, the Transverse Ising Model has been used to represent enormous simple-to-complex systems such as brain science and information science and technology.

We consider the 1D Transever Ising ring, describing the nearest neighbor interactions of the spin projection along the z-axis and uniform external magnetic field along the x-axis (in principle, perpendicular to the z-axis). Defined by the two spin exchange interaction factor J and representative strength of the external field h as described below

$$\hat{H}_{\text{TIM}} = -J \sum_{n=1}^{N-1} \sigma_{n-1}^z \sigma_n^z - h \sum_{n=0}^{N-1} \sigma_n^x. \qquad (4)$$

The Hamiltonian in Eq. (4) possesses a $\mathbf{Z}_2$ symmetry remaining invariant under spin flipping action. When the coupling constant $h < 1$, the system exhibits a ferromagnetic phase, the spins favorably align along the z-direction. Conversely, for $h > 1$, the system transitions to a disordered paramagnetic phase. The σ_x terms take a dominant rule when $h \to \infty$, leading the ground state to align predominantly in the $|+\rangle^{\otimes N}$ state. At the critical point $h = 1$ renders the gapless property in the thermodynamic limit.

One of the key differences between the classical and quantum versions of the Ising model is that the expectation value of two terms in the Eq. (4) must be measured twice due to the non-commutative feature of these elements. The first term can be cumulatively achieved by measuring directly on the computational basis as follows:

$$\langle \sigma_m^z \sigma_n^z \rangle = \sum_{\{q_0, \cdots, q_{N-1}\} = \{0,1\}} |a_{q_0 \cdots q_m \cdots q_n \cdots q_{N-1}}|^2 (-1)^{q_m + q_n},$$
$$(5)$$

$$\langle \sigma_n^z \rangle = \sum_{\{q_0, \cdots, q_{N-1}\} = \{0,1\}} |a_{q_0 \cdots q_n \cdots q_{N-1}}|^2 (-1)^{q_n}, \qquad (6)$$

with $|a_{q_0 \cdots q_m \cdots q_n \cdots q_{N-1}}|^2$ and $|a_{q_0 \cdots q_n \cdots q_{N-1}}|^2$ are the probability of being in the computational basis state $|q_0 \cdots q_m \cdots q_n \cdots q_{N-1}\rangle$ and $|q_0 \cdots q_n \cdots q_{N-1}\rangle$ respectively. Similarly, $\sum_{n=0}^{N-1} \sigma_n^x$ is obtained by applying the Hardamard gate or the $R_y\left(-\frac{\pi}{2}\right)$ gate in advance to transform to the Z-basis, or computational basis, and then taking the measurements following Eq. (6).

B. Ansatz Construction

To construct an ansatz in terms of parameterized quantum circuit (PQC), as mentioned above, we need the $U(\boldsymbol{\theta})$ operator can span all quantum Hilbert space so that we can use to solve all issues. Indeed, we do not, in practice though, a general $U(\theta)$ operator is hard to implement experimentally, because of noisy and weighty composite $C - U_3$ gate, and actually does not acquire overall good operation even in an ideal simulator. Hence, the ansatz implementation for a particular problem's purpose is a serious studying process of the VQE working roadmap. In addition to the compatibility with the current quantum device, tapping into symmetries and properties of our problem could be leveraged to shrink the parameter space, which are the important criteria for adopting an ansatz.

1. Symmetry of Transverse Ising model

At the scope of this article, we consider three properties of TIM so that we take its suggesting information into account to decrease the size of ansatz

- *Real representation.* Using the eigenstates of the σ_Z (Pauli-z) operator as the elementary binary computational basis, in terms of which, σ^z, σ^x are real matrices, due to that, we can represent the TIM Hamiltonian in the real form, the eigenstates of TIM Hamiltonian can thus choose to be real for conventional. Namely, considering $|\Psi\rangle = \sum_n C_n|n\rangle$ is a eigenstate of H_{TIM} expanding in the computational basis $|n\rangle$. The real form of H_{TIM} means the Hermitian real element matrix, that induces coefficients satisfied $C_n^* C_m = C_n C_m^* \; \forall m, n \in [0, 2^N - 1]$, then, in generality

$$C_n = r_n e^{i(c + k_n \pi)}, \quad c \text{ is a constant}, \quad (7)$$

or, in other words, the angles in the complex plane of coefficients C_n differ from every other by a factor $k\pi$, where k and k_n are integers. Then, the complex angle can be shifted to the real coefficient $C_n^* = C_n$ by according to the quantum global phase principle.

- *Local interaction.* The first term $\hat{H}_{\text{TIM}}^{\text{LI}}$ in TIM Hamiltonian describing the kind of neighbouring spin interaction along the z-axis

$$\hat{H}_{\text{TIM}}^{\text{LI}} = \sum_{n=1}^{N-1} \sigma_{n-1}^z \sigma_{n+1}^z. \quad (8)$$

The interaction of two local spin formulating by this term causes a sort of entanglement structure between every two local spin of the ground state energy. nevertheless, in the case of the order phase, when the external magnetic field is dominant, this interaction can be broken down, each spin will be free interacting and align in the same direction of the magnetic field.

- *Total spin-flip symmetry .* The most featured symmetry of Ising model, can be referred to the classical counterpart, Time-reversal symmetry (generally, $\mathcal{Z}_2$ symmetry). Under the total spin-flip transformation in the z direction $(\sigma^x)^{\otimes N}$

$$\left[(\sigma^x)^{\otimes N}, \hat{H}_{\text{TIM}} \right] = 0, \quad (9)$$

which implies the TIM Hamiltonian remains unchanged. This one leads to the eigenstate $|\Psi\rangle$ and $(\sigma^x)^{\otimes N} |\Psi\rangle = |\tilde{\Psi}\rangle$ have the same energy, the relation between them thus put in two cases

$$\langle \Psi | \tilde{\Psi} \rangle = \begin{cases} 0 & \text{Degeneracy} \\ \pm 1 & \text{Non-degeneracy} \end{cases}, \quad (10)$$

where, degenerate case $g = 0$ is trivial, at non-degenerate $g > 0$ case, the expanded coefficients in the z-direction basis representation having a structure

$$C_n = \pm C_{2^N - 1 - n}. \quad (11)$$

2. Ansatz selection

For the chosen ansatz, the conventional real coefficients of eigenstates tell us that is enough to span in a real quantum parameter space for finding the ground state energy, and the linear entanglement mapping coming from information of the local interaction term in Hamiltonian. Moreover, to accommodate the device constraints, in speculative way, basing on these conditions, the available common use RealAmplitude ansatz from Qiskit open source is our good candidate for the implementation.
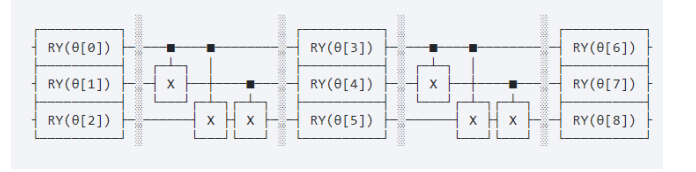

FIG. 2: A RealAmplitudes circuit with 2 repetitions on 3 qubits with 'full' entanglement

The additional reason for choosing such a Hardware-efficient ansatz [10] comes from the efficient implementation of quantum optimization to attain our full quantum algorithm purpose, which will be addressed in the next subsection IV B.

For efficiently traveling around full quantum Hilbert space we need to tune $2^{N+1} - 2$ degrees of freedom, $+1$ inside of the exponent indicates the complex number condition, and -2 turns up from normalization and global phase conditions. After bringing TIM's properties we investigate from section III B 1 to dissect, *Real representation* Eq. (7) helps us eliminate $+1$ within the exponent and *Total spin-flip symmetry* Eq. (11) reduces a half as much numbers of parameters that we have to search the ground state, finally

$$2^{N+1} - 2 \rightarrow 2^{N-1} - 1. \quad (12)$$

The factor *repetition (reps)* of our RealAmplitude ansatz is used to modify number of layer L, which changes directly ansatz number of parameter p according to $p = N(L + 1)$. Following Eq. (12), we roughly evaluate a necessary number of layer

$$L \geq \frac{2^{N-1} - 1}{N} - 1, \quad (13)$$

note that this is not a rigorous condition because ansatz's entanglement mapping scheme used also contributes,

which is able to change the bound as well, it is still a good estimation for surface analysis nonetheless. Yet, we can realize that, not only TIM, but Eq. (12) also holds for all symmetrically real Hamiltonian being symmetric under $(\sigma^x)^{\otimes N}$ operator. Therefore, there are some hidden TIM properties that we are unable to analytically incorporate to give an exact boundary value of L, through conducting the experimental survey though, we are able to choose a reliable value for L.

IV. OPTIMIZATION

The next subroutine in VQE work map, which is a purely technical perspective we investigate to study the performance of different optimization methods, provides us a larger view of the way to reaching the faster and more precise convergence of our target value. In TIM, we try to minimize the cost function defined as expectation value of Hamiltonian $\langle \hat{H}_{\text{TIM}} \rangle$ using common methods of optimization categorized into two class operations.

A. Classical Operation

Classical operation means regardless of the analysis quantum structure of cost function, in particular ansatz structure, we are able to find the optimal parameters minimizing the objective function. Normally, in sense of operation, we can do the classical optimization process independently from each other VQE parts and even with your problem-specific concerns, and appears that you can develop your optimization algorithm for general variational issues.

Constrained Optimization BY Linear Approximation (COBYLA). One of the most powerful derivative free methods, which is favoured by many users in lately decades, COBYLA makes use of linear interpolation of the objective function at each iteration by a unique linear polynomial function at the vertices for finding a optimal vector parameter within the trust region, then feeding optimal point evaluated to the objective function to get the value improving the next iteration of approximation [11–14]. In VQE, COBYLA's linear interpolation at each step is a classical subroutine running on CPU using only one the objective value from QPU evaluation running. And so because of ignored derivative information, it would beneficially avoid several problems in analysis optimizations, especially Barren plateaus landscape, in return less accuracy for more parameters ($p > 9$) [14]. For a bird-eye view, new update COBYLA versions like UOBYQA, NEWUOA, and BOBYQA count the objective function's curvature information to increase convergence [15–17].

Finite Difference (FD). Let's dawn on one of the primary first-order derivative-based approaches, where the parameter $\boldsymbol{\theta} \in \mathbb{R}^p$ is updated at the iteration k-th by

$$\boldsymbol{\theta}_{k+1} = \boldsymbol{\theta}_k - \eta_k \nabla f(\boldsymbol{\theta}_k), \qquad (14)$$

which we usually name the Gradient Descent (GD) method. Finite Difference is a numerical technique to calculate the gradient vector $\nabla f(\boldsymbol{\theta}_k)$ without the analytical function's texture, which is the basic one used in the gradient descent method. We use the well-known central difference formula

$$\nabla f(\boldsymbol{\theta}_k)_i \simeq \frac{f(\boldsymbol{\theta}_k + \epsilon \vec{i}) - f(\boldsymbol{\theta}_k - \epsilon \vec{i})}{2\epsilon}, \qquad (15)$$

where $\vec{i} \in \mathbb{R}^p$ is i-th the unit vector and ϵ is an infinitesimal change, with the error proportional to $\mathcal{O}(\epsilon^2)$. The smaller ϵ we use, the more exact result we get. However, due to the restricted accuracy of a classical computer, we are unable to achieve a value of ϵ that is too small, which even becomes greater when implemented on a quantum device, where at least the sample error enters the picture.

Simultaneous Perturbation Stochastic Approximation (SPSA). To surmount some of obstacles emerge from gradient descent operation on near-term device, the idea of a perturbing stochastic approximation method is a good choice. SPSA generates an unbiased estimator $\tilde{f}(\boldsymbol{\theta}_k)$ of gradient by simultaneously radomly perturbating gradient direction of parameters [18], we replace the ordinary gradient vector $\nabla f(\boldsymbol{\theta}_k)$ by

$$\nabla f(\boldsymbol{\theta}_k) \rightarrow \nabla \tilde{f}(\boldsymbol{\theta}_k) = \frac{f(\boldsymbol{\theta}_k + s_k \vec{\Delta}_k) - f(\boldsymbol{\theta}_k - s_k \vec{\Delta}_k)}{2s_k} \vec{\Delta}_k, \qquad (16)$$

where $\vec{\Delta}_k$ is a random perturbed vector sampled from the zero-mean distribution, usually, the Bernoulli distribution is used. We can see that all parameters are simultaneously shifted by a random amount ($\pm s_k$), our computation therefore only requires two objective function evaluations per iteration. Whereas standard gradient computation time is scaled along to number of parameters, the SPSA optimizer is, however, independent, that saves a lot of time as we work on higher parameter regime. Besides that, noise from quantum circuit executions computing the objective value be regarded as a stochastic perturbation part absorbed to the SPSA procedure. These advantages promote SPSA and its other version to be efficient techniques in the NISQ era.

B. Quantum Operation

As opposed to classical one, the quantum operation require the quantum information extracted from the structure of the trial wave function. This sort of behaviour inevitably entails the optimization process into to whole problem analysis, especially related close to Ansatz Construction.

Parameter-shift rules (PSR). Inspiring from the classical shift rules in the exact derivative computation of some special function, we are successfully able to figure out the analytical value of objective function's derivatives using

quantum devices. For any kinds of quantum gates have the form

$$\hat{\mathcal{G}}(\theta) = e^{-i\theta\hat{G}} \qquad (17)$$

generated by the Hermitian operator $\hat{G}$. Supposed that we have an expectation value of $\hat{H}$ is our objective function $f(\theta) = \langle\psi(\theta)|\hat{H}|\psi(\theta)\rangle$ parametrized by θ. The ansatz wave function $|\psi(\theta)\rangle = \hat{U}(\theta)|\psi\rangle_I$ is made up of $\hat{U}(\theta) = \hat{A}\hat{\mathcal{G}}(\theta)\hat{B}$, with $\hat{A}$, $\hat{B}$ are arbitrarily other operators. As a result, the partial derivative of the $f(\theta)$ with respect to θ is thus obtained via the parameter-shift rules [19]

$$\partial_\theta f(\theta) = s\left[f(\theta + \frac{\pi}{4s}) - f(\theta - \frac{\pi}{4s})\right]. \qquad (18)$$

The partial derivative $\partial_\theta = \frac{\partial}{\partial\theta}$ implies we can generalize to set of multiple parameters $\{\theta_i\}$. The evaluation of $f(\theta \pm \frac{\pi}{4s})$ can be easy to run on quantum computer, then the exact amplitude of vector gradient is derived. Within the aim of this paper, the given parametric ansatz is made out of Pauli rotations, $s = \frac{1}{2}$ is selected accordingly. The state of the art formalism for more generic PQCs are also able to be derived [20, 21].

Quantum Natural Gradient Descent (QNG). How to improve the convergence? The global fixed learning rate η_k is apparently not a good choice, one does not be well sensitive to the model information with respect to parameter changes. Initially, many attempts try to tune the learning rate η_k such as learning rate schedulers that vary η_k after an iteration, laterly, adaptive methods that count previous iteration values, or capturing the curvature of the objective function using the diagonal approximation of the Hessian, where each η_k is the inverse Hessian's diagonal element instead of being equally fixed. Those methods educe that a we can embed further information rather than only just gradient vector, to make the optimal step size for our variational quantum algorithms. Likewise, the classical counterpart using Fisher Information matrix (FIM), Quantum Natural Gradient Descent invokes the quantum geometry of the wave function, which can make us get the optimal spot faster. Namely, we transform to the Riemann parameter space using metric $g \in \mathbb{R}^{p \times p}$ of Projected Hilbert space $\mathcal{PH}$ instead of current Euclidean space $g = \mathbb{1}_{p \times p}$. The update Eq. (14) turns to

$$\boldsymbol{\theta}_{k+1} = \boldsymbol{\theta}_k - \eta_k g^+(\boldsymbol{\theta}_k)\nabla f(\boldsymbol{\theta}_k), \qquad (19)$$

$g^+(\boldsymbol{\theta}_k)$ means it is a pseudo-inverse local metric. Riemann parameter space metric g is generally defined

$$ds^2 = g_{ij}d\theta_i d\theta_j. \qquad (20)$$

The Hilbert space $\mathcal{H}$ of "bare" quantum states reduces to the $\mathcal{PH} = \mathcal{H}/U(1)$ space as we ignore the local phase $U(1)$ of quantum states [22], the quantum distance in $\mathcal{PH}$

is then based on to calculate the Riemann metric g

$$\begin{aligned} ds^2 &= 1 - |\langle\psi_\theta, \psi_{\theta+d\theta}\rangle|^2 \\ &= 1 - \left|1 + \frac{1}{2}\langle\psi_\theta|\partial_i\partial_j\psi_\theta\rangle d\theta_i d\theta_j + \langle\psi_\theta|\partial_i\psi_\theta\rangle d\theta_i\right|^2 \\ &= \text{Re}[G_{ij}]d\theta_i d\theta_j. \end{aligned} \qquad (21)$$

We expand $|\psi_{\theta+d\theta}\rangle = |\psi_\theta\rangle + |\partial_i\psi_\theta\rangle d\theta_i + \frac{1}{2}|\partial_i\partial_j\psi_\theta\rangle d\theta_i d\theta_j$ upto second order in $d\theta$, where $\partial_i = \frac{\partial}{\partial\theta_i}$. The Quantum Geometry tensor (QGT) $G_{ij} \in \mathbb{R}^{p \times p}$ has two parts, the anti-symmetric imaginary part $\sigma_{ij} = -\sigma_{ji}$ related to gauge field of $U(1)$ is eventually vanished, the only contribution comes from the real symmetric part $g_{ij} \equiv g_{ij}(\boldsymbol{\theta})$ reflects the quantum distance in $\mathcal{PH}$ space, where its formula is

$$g_{ij}(\boldsymbol{\theta}) = \text{Re}\left[\langle\partial_i\psi_\theta|\partial_j\psi_\theta\rangle - \langle\partial_i\psi_\theta|\psi_\theta\rangle\langle\psi_\theta|\partial_j\psi_\theta\rangle\right]. \qquad (22)$$

The Fubini-Study metric tensor $g_{ij}(\boldsymbol{\theta})$ is a quantum analogue of the Fisher information matrix (QFIM). Given that it is proportional to p^2, the complicated computing and computational cost of $g(\boldsymbol{\theta})$ is high and incompatible with the short-term quantum device. To solve this problem, an approximation strategy is required.

- *QNG - Block Diagonal Approximation (QN-BDA).* Moreover than Diagonal Approximation, where we just count p elements in diagonal line, the QNG-BDA employing the Parametric Family circuit is conveniently deploy entirely computation of approximated metric tensor on the quantum computer. The parametric unitary operator $\hat{U}(\boldsymbol{\theta})$ acts on the initial state $|\psi\rangle_I$ entailing L layers

$$\hat{U}(\boldsymbol{\theta}) = S_L P_L(\theta^L)\ldots S_1 P_1(\theta^1), \qquad (23)$$

where:

  - S_l are the static parts, which usually denote to the entanglement layer.
  - $P_l(\theta^l)$ are the parametric parts, which can be decomposed to single qubit gates $P_l(\theta^l) = \bigotimes_{i=1}^{N} R_i(\theta_i^l)$.
  - The single qubit gate $R_i(\theta_i^l) = \exp\{[i\theta_i^l K_i]\}$ is constructed from Hermitian generator K_i with the parameter $\theta_i^l \in \theta^l = \{\theta_1^l, \ldots, \theta_N^l\}$.

Such type of parametrized circuit whose nice properties we can prospect to yield a block diagonal form of QGT running completely on quantum processor, each block corresponding to each layered vector parameter $\theta^l \in \boldsymbol{\theta} = \theta^1 \oplus \ldots \oplus \theta^L$. We denote

$$\hat{U}_n^m = S_m P_m(\theta^m)\ldots S_n P_n(\theta^n), \qquad (24)$$

then $\hat{U}(\boldsymbol{\theta}) \equiv \hat{U}_1^L = \hat{U}_{l+1}^L S_l P_l(\theta^l)\hat{U}_1^{l-1}$. The partial

derivative state can be written in form

$$|\partial_i \psi_\theta\rangle = \partial_i \hat{U}(\boldsymbol{\theta})|\psi\rangle_I \tag{25}$$

$$= \hat{U}_{l+1}^L S_l \partial_i P_l(\theta^l) \hat{U}_1^{l-1} |\psi\rangle_I \tag{26}$$

$$= \hat{U}_l^L (iK_i) \hat{U}_1^{l-1} |\psi\rangle_I \tag{27}$$

$$= \hat{U}_l^L (iK_i) |\psi_\theta^{(l-1)}\rangle. \tag{28}$$

Note that $[K_i, K_j] = 0$ in each layer, the unitarity of $\hat{U}_n^m$ and overlap of partial derivative states tell us the block matrix element

$$g_{ij}^{(l)}(\boldsymbol{\theta}) = \langle \psi_\theta^{(l-1)} | K_i K_j | \psi_\theta^{(l-1)} \rangle \\ - \langle \psi_\theta^{(l-1)} | K_i | \psi_\theta^{(l-1)} \rangle \langle \psi_\theta^{(l-1)} | K_j | \psi_\theta^{(l-1)} \rangle \tag{29}$$

of block-diagonal form of Fubini-Study metric [23]

$$g_{ij}(\boldsymbol{\theta}) = \begin{array}{c} \\ \theta^1 \\ \theta^2 \\ \\ \vdots \\ \\ \theta^L \end{array} \begin{array}{cccc} \theta^1 & \theta^2 & \dots & \theta^L \\ \begin{pmatrix} g^{(1)} & 0 & \dots & 0 \\ 0 & g^{(2)} & \dots & 0 \\ \vdots & \vdots & \ddots & \vdots \\ 0 & 0 & \dots & g^{(L)} \end{pmatrix} \end{array}. \tag{20}$$

QNG-BDA approximation involves L quantum evaluations and works well on models with weak correlation.

Quantum Natural-Simultaneous Perturbation Stochastic Approximation (QN-SPSA). Inheriting the SPSA idea to calculate the gradient, it is capable to put up to generate the Hessian matrix with fewer evaluations, the so-call 2-SPSA. Normally, the Hessian or FIM matrix consumes $\mathcal{O}(p^2)$ quantum expectation, QNG-BDA enables us turn to relying on number of layer $\mathcal{O}(L)$, saving us lots of computational sources. Even further, QN-SPSA just only execute four quantum running to obtain full of the second order derivative matrix. Let's consider the Hessian of the Fubini-Study metric

$$H_{ij}(\boldsymbol{\theta}) \equiv g_{ij}(\boldsymbol{\theta}) = - \frac{1}{2} \partial_i \partial_j |\langle \psi_\theta, \psi_{\tilde{\theta}} \rangle|^2 \Big|_{\tilde{\theta}=\theta}, \tag{30}$$

which is just Hessian form of Eq. (22) so that we can deploy the 2-SPSA method to generate QN-SPSA matrix. We can see the equivalence

$$- \frac{1}{2} \partial_i \partial_j |\langle \psi_\theta, \psi_{\tilde{\theta}} \rangle|^2 \Big|_{\tilde{\theta}=\theta} = -\partial_i \text{Re} \left\{ \langle \psi_\theta, \psi_{\tilde{\theta}} \rangle \langle \psi_{\tilde{\theta}}, \partial_j \psi_\theta \rangle \right\} \Big|_{\tilde{\theta}=\theta}$$
$$= -\text{Re} \left\{ \langle \psi_\theta, \partial_i \partial_j \psi_\theta \rangle + \langle \partial_i \psi_\theta, \psi_\theta \rangle \langle \psi_\theta, \partial_j \psi_\theta \rangle \right\}$$
$$= -\text{Re} \left\{ -\langle \partial_i \psi_\theta, \partial_j \psi_\theta \rangle + \langle \partial_i \psi_\theta, \psi_\theta \rangle \langle \psi_\theta, \partial_j \psi_\theta \rangle \right\}, \tag{31}$$

which is exactly same as Eq. (22). Applying 2-SPSA approach to compute second order derivative of function $F(\boldsymbol{\theta}, \tilde{\theta}) = -\frac{1}{2} |\langle \psi_\theta, \psi_{\tilde{\theta}} \rangle|^2$ instead of our loss function $f(\boldsymbol{\theta})$ as being in Newton method. The core estimator in

second-order SPSA is perturbed by two random vectors $\vec{\Delta}_k^1, \vec{\Delta}_k^2 \in \mathcal{U}^p\{-1, 1\}$ at step k-th

$$\triangle F = \frac{-1}{2} \Big[F(\boldsymbol{\theta}_k + s_k \vec{\Delta}_k^1 + s_k \vec{\Delta}_k^2, \boldsymbol{\theta}_k) \\ -F(\boldsymbol{\theta}_k + s_k \vec{\Delta}_k^1, \boldsymbol{\theta}_k) + F(\boldsymbol{\theta}_k - s_k \vec{\Delta}_k^1, \boldsymbol{\theta}_k) \\ - F(\boldsymbol{\theta}_k - s_k \vec{\Delta}_k^1 + s_k \vec{\Delta}_k^2, \boldsymbol{\theta}_k) \Big], \tag{32}$$

which is composed of four terms respective to four quantum expectations we run on quantum processor. Then, the Fubini-Study metric Eq. (30) is replaced by QN-SPSA metric at k-th iteration

$$g^k(\boldsymbol{\theta}) \to \bar{H}^k(\boldsymbol{\theta}) = \frac{\triangle F}{4s_k^2} \left(\vec{\Delta}_k^1 \vec{\Delta}_k^{2\text{T}} + \vec{\Delta}_k^2 \vec{\Delta}_k^{1\text{T}} \right), \tag{33}$$

where $\bar{H}^k(\boldsymbol{\theta}) \in \mathbb{R}^{p \times p}$ and s_k is a small positive hyperparameter being able to be tuned. The metric is, however, still too much stochastic, some helpful techniques is invoked to resolve that hitch [24, 25], say, counting information from previous updates to smooth the estimator

$$\tilde{H}^k = \frac{k}{k+1} \tilde{H}^{k-1} + \frac{1}{k+1} \bar{H}^k, \tag{34}$$

eventually, because the estimator still be ill-conditioned and unstable, to satisfy the positive semi-definite warranting the local convex analysis and invertibility condition of $\tilde{H}^k$, the below replacement is needed respectively

$$\tilde{H}^k \to \sqrt{\tilde{H}^k \tilde{H}^k} + \beta \mathbb{1}, \tag{35}$$

where the second term $\beta \mathbb{1} \in \mathbb{R}^{p \times p}$ corresponds to invertibility condition. The effect from geometry metric is suppressed as the positive regulator gets a huge value $\beta \gg 0$, that is indeed standard gradient descent, and be more unstable, which means larger deviation in the average sample result, when $\beta \to 0$. That makes constant regulator β is thus a trade-off between Quantum Natural information and numerical instability. Another regularization approach, called "half-inversion", generalizes the power of the second-order derivative matrix to n instead of the usual ones -1 corresponding to standard natural gradient and 0 standing for original gradient, given by [26].

The Quantum Natural Gradient SPSA with Parameter-Shift Rule (QN_SPSA -PSR) is our extension for QN_SPSA-SPSA method. Although QN_SPSA-SPSA has smaller complexity when compared with other methods, this stochastic method seems so randomized and made it harder to converge and less stable when it comes to a bigger cost function landscape. Here, We propose the QNSPSA-PSR algorithm, which is inherent in approximating the Fubini-Study metric properties in way of saving computational cost, however, instead of using the SPSA method to approximate the gradient of the cost function, we use the analytical method to calculate the gradient by PSR, this is expected for more stable and fast convergence, compared to the former method QN_SPSA-SPSA.
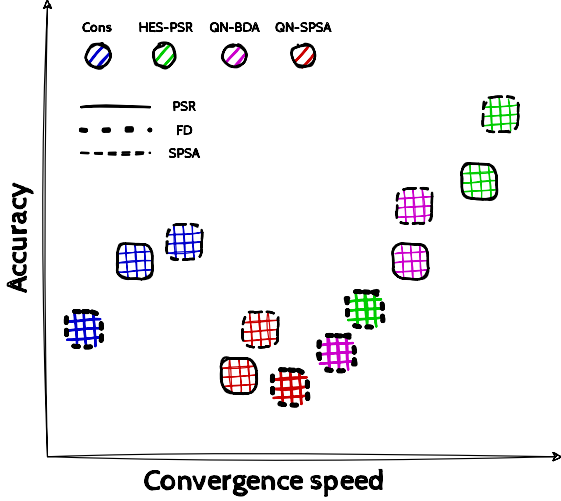
FIG. 3: The comparative graphics among combinations of gradient and adaptive learning rate methods

V. RESULTS AND CONCLUSION

A. Complexity estimation

Derivative-based method efficiency			
$\nabla f(\boldsymbol{\theta})$	PSR	FD	SPSA
Comp. cost	2p	2p	2
$g(\boldsymbol{\theta})$	Hes-PSR	QNG-BDA	QN-SPSA
Comp. cost	3p.p	L	4

TABLE I: Showing comparison among combinations of gradient and adaptive learning rate methods. Where p is the number of parameters, L is the number of PQC layers of the same rotation generator.

We provide a roughly assessment of the optimization methods, grounded in theoretical judgment, where you are able to read off their information from Tab. I or Fig. 3 for more illustrative, that contains computational cost, accuracy, and convergence speed. A method is a combination of gradient and adaptive learning rate, such as QN-BDA + PSR which is estimated the computational cost is L*2p. That means this method is almost highly accurate, just following behind Hes-PSR + PSR, and only slower than Hes-PSR + PSR (FD) in terms of convergence speed. Hes-PSR here is the Hessian (Hes) matrix computed by the Parameter Shift Rule (PSR) in second order, and Const is the constant learning rate.

We also conducted the ansatz comparison, which is presented in Fig. 5. Here we used RealAmplitude (Re-alAmp) ansatz and Efficient SU2 (EFFSU2) ansatz with the linear entanglement mapping. It turned out that the RealAmp performed better in convergence. As aforementioned in the section III B 2, the RealAmp therefore is good enough to survey the Ising model space.

The final result of the optimization ansatz comparison is shown in Fig. 4. Based on the Tab. I, we additionally implemented two methods QNG-BDA + SPSA and QN-SPSA + PSR shortened as QN_SPSA and QN-SPSA_PSR respectively in Fig. 4. The result displays an exciting outcome, although the QN_SPSA is not stable with the large uncertainty, it showed up a potential accuracy as it is able to reach the better optimal solution compared to the other methods. Meanwhile, the QN_SPSA is more stable than its cousin QNSPSA_SPSA (QN-SPSA+SPSA) where we replaced the SPSA method with the QN-BDA to compute the Fubini metric, which in turn comes off with less attractive due to its poor precision.

B. Simulation results

We simulate the VQE with various optimizations, the amount of spin in the TIM model, and different ansatz. Remember that, if not specified, the default values are $h = 2$ and $J = 1$ for the external field and exchanged coupling, respectively. For the stochastic method, I would sample seven of them, and these optimizations would be evaluated based on all of their samples. The source code can be found at https://github.com/linhhacoV-I-P/Variational-Quantum-EigeinSolver. In Fig. 4, we use the RealAmplitudes ansatz, reversed-linear entanglement with one repetition, to compare six different optimizations: SPSA, QN_PSR, Finite Difference, Cobyla, QNSPSA_PSR, and QNSPSA_SPSA. At theoretical prediction, QN_PSR method has the fastest convergence by leveraging the Fubini-Study metric tensor. Significantly, QNSPSA_PSR outperforms Cobyla and Finite Difference methods. By a small change in the gradient part from stochastic estimation to exact, we improve the performance of the inspired QNSPSA _ SPSA method, which made QNSPSA_PSR more stable and faster convergence.

Then, we compared further with the more complex hardware efficient ansatz: EfficientSU2 in Fig. 5. Although EfficientSU2 ansatz would create a more complex cost function, QNSPSA_PSR still shows stable and fast convergence properties and sometimes can compare with QN_PSR optimization. Whereas, QNSPSA_SPSA and Cobyla are stuck and need more interaction to find the global optimum point

Moreover, We extend our evaluation with QNSPSA_PSR method by estimating the average ground state energy with various circumstances with QNSPSA_SPSA and QN_PSR optimization in Figs. 6 and 7. In both cases, we observed a better result in terms of energy estimate and more reliability than QNSPSA_SPSA. Additionally, in all cases, the
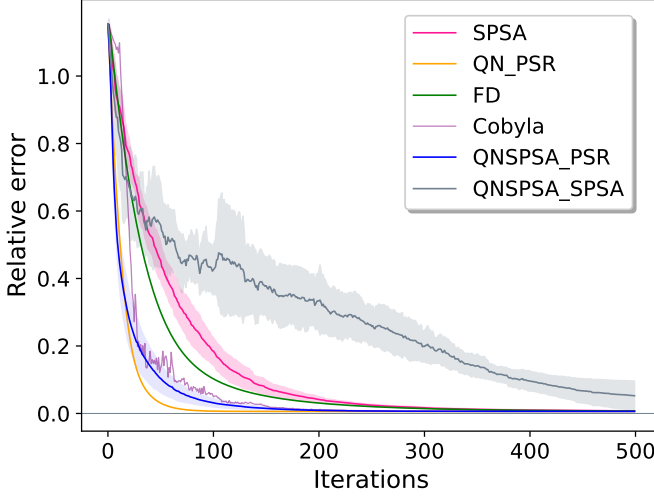
(a) Linear entanglement mapping
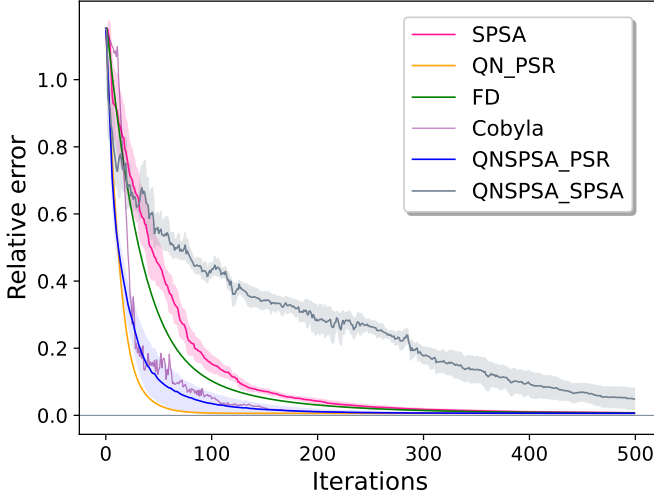
(b) Full entanglement mapping

FIG. 4: Comparing multiple optimizations of TIM's 12 spins with RealAmplitudes Ansatz

QNSPSA_PSR can converge to the average ground state energy that QN_PSR does.

C. Conclusion

In conclusion, this research delved into the analysis of the Ising Model, leveraging the model's properties and symmetries to conjecture an ansatz form. Subsequently, a review of optimization algorithms was conducted, comparing the trade-offs between quantum and classical algorithms to provide a bird's eye view.

The results of the running indicated that the chosen ansatz form, based on the Hamiltonian's properties, performed reasonably well, despite estimating the number of layers in Eq. 13 does not work in this case. However, it is
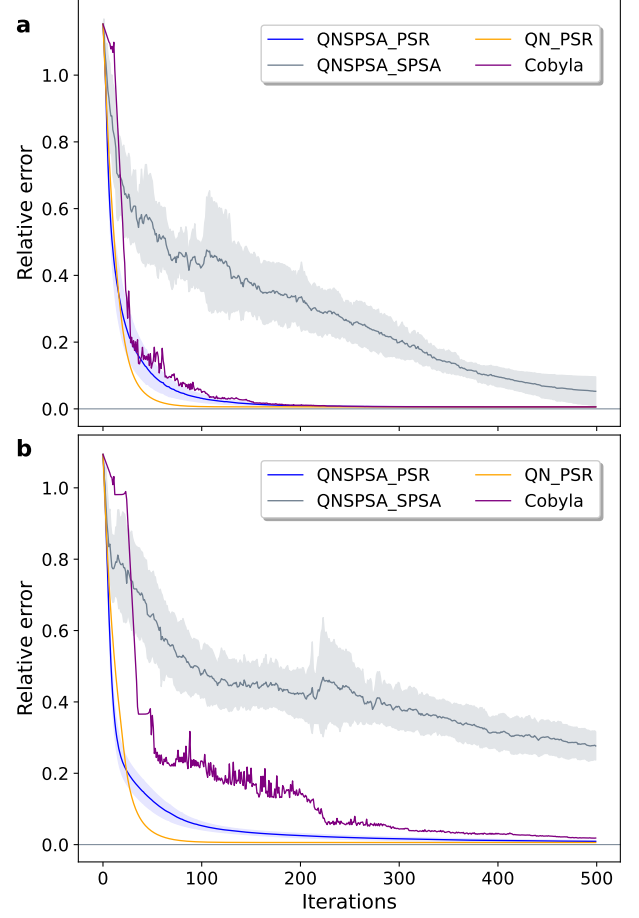

FIG. 5: Comparing multiple optimizations of TIM's 12 spins with a) RealAmplitudes Ansatz and b) EfficientSU2 Ansatz
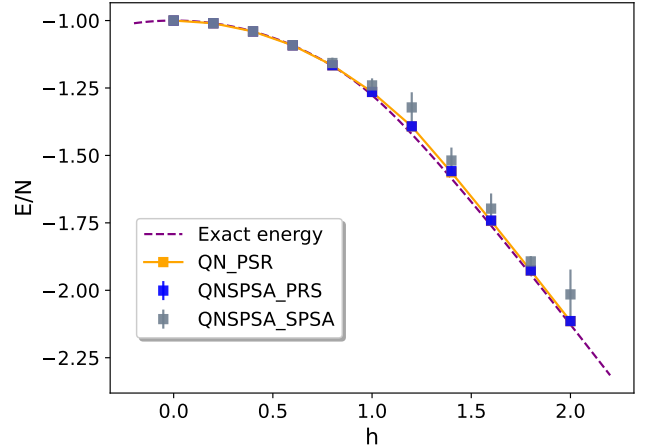

FIG. 6: Estimate the average ground state energy with QNSPSA_SPSA, QNSPSA_PSR and QN_PSR for TIM of 12 spins and different external fields with RealAmplitudes ansatz
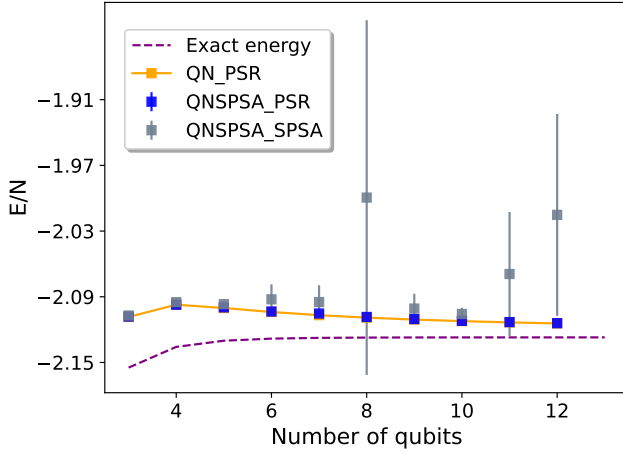
FIG. 7: Estimate the average ground state energy with QNSPSA SPSA, QNSPSA PSR, and QN PSR for TIM of different spins with RealAmplitudes ansatz

believed to serve as a reasonably good initial estimation as the system scales up.

Lastly, the combined algorithm QNSPSA_PSR exhibited unexpected theoretical prediction by demonstrating potential not only in reducing computational costs, as it does not scale up significantly with qubits like traditional Quantum Natural methods, but also in achieving more accurate optimal solutions. This suggests promising prospects for further exploration and application of such algorithms in future research endeavors.

[1] F. Arute, K. Arya, R. Babbush, D. Bacon, J. C. Bardin, R. Barends, R. Biswas, S. Boixo, F. G. Brandao, D. A. Buell, *et al.*, Quantum supremacy using a programmable superconducting processor, Nature **574**, 505 (2019).

[2] A. Peruzzo, J. McClean, P. Shadbolt, M.-H. Yung, X.-Q. Zhou, P. J. Love, A. Aspuru-Guzik, and J. L. O'brien, A variational eigenvalue solver on a photonic quantum processor, Nature communications **5**, 1 (2014).

[3] J. R. McClean, J. Romero, R. Babbush, and A. Aspuru-Guzik, The theory of variational hybrid quantum-classical algorithms, New Journal of Physics **18**, 023023 (2016).

[4] J. Tilly, H. Chen, S. Cao, D. Picozzi, K. Setia, Y. Li, E. Grant, L. Wossnig, I. Rungger, G. H. Booth, *et al.*, The variational quantum eigensolver: a review of methods and best practices, arXiv preprint arXiv:2111.05176 (2021).

[5] K. Bharti, A. Cervera-Lierta, T. H. Kyaw, T. Haug, S. Alperin-Lea, A. Anand, M. Degroote, H. Heimonen, J. S. Kottmann, T. Menke, *et al.*, Noisy intermediate-scale quantum (nisq) algorithms, arXiv preprint arXiv:2101.08448 (2021).

[6] E. Grant, M. Benedetti, S. Cao, A. Hallam, J. Lockhart, V. Stojevic, A. G. Green, and S. Severini, Hierarchical quantum classifiers, npj Quantum Information **4**, 10.1038/s41534-018-0116-9 (2018).

[7] G. Carleo and M. Troyer, Solving the quantum many-body problem with artificial neural networks, Science **355**, 602 (2017), https://www.science.org/doi/pdf/10.1126/science.aag2302.

[8] X. Bonet-Monroig, R. Babbush, and T. E. O'Brien, Nearly optimal measurement scheduling for partial tomography of quantum states, Phys. Rev. X **10**, 031064 (2020).

[9] D. Wang, O. Higgott, and S. Brierley, Accelerated variational quantum eigensolver, Physical Review Letters **122**, 10.1103/physrevlett.122.140504 (2019).

[10] A. Kandala, A. Mezzacapo, K. Temme, M. Takita, M. Brink, J. M. Chow, and J. M. Gambetta, Hardware-efficient variational quantum eigensolver for small molecules and quantum magnets, Nature **549**, 242 (2017).

[11] M. J. D. Powell, Direct search algorithms for optimization calculations, Acta Numerica **7**, 287–336 (1998).

[12] M. J. Powell, A view of algorithms for optimization without derivatives, Mathematics Today-Bulletin of the Institute of Mathematics and its Applications **43**, 170 (2007).

[13] A. R. Conn, K. Scheinberg, and P. L. Toint, On the convergence of derivative-free methods for unconstrained optimization, Approximation theory and optimization: tributes to MJD Powell , 83 (1997).

[14] M. J. Powell, A direct search optimization method that models the objective and constraint functions by linear interpolation, in *Advances in optimization and numerical analysis* (Springer, 1994) pp. 51–67.

[15] M. J. Powell, Uobyqa: unconstrained optimization by quadratic approximation, Mathematical Programming **92**, 555 (2002).

[16] M. J. Powell, The newuoa software for unconstrained optimization without derivatives, in *Large-scale nonlinear optimization* (Springer, 2006) pp. 255–297.

[17] M. J. Powell, The bobyqa algorithm for bound constrained optimization without derivatives, Cambridge NA Report NA2009/06, University of Cambridge, Cambridge **26** (2009).

[18] J. C. Spall, An overview of the simultaneous perturbation method for efficient optimization, Johns Hopkins apl technical digest **19**, 482 (1998).

[19] M. Schuld, V. Bergholm, C. Gogolin, J. Izaac, and N. Killoran, Evaluating analytic gradients on quantum hardware, Physical Review A **99**, 10.1103/physreva.99.032331 (2019).

[20] L. Banchi and G. E. Crooks, Measuring Analytic Gradients of General Quantum Evolution with the Stochastic Parameter Shift Rule, Quantum **5**, 386 (2021).

[21] D. Wierichs, J. Izaac, C. Wang, and C. Y.-Y. Lin, General

parameter-shift rules for quantum gradients, Quantum **6**, 677 (2022).

[22] R. Cheng, Quantum geometric tensor (fubini-study metric) in simple quantum system: A pedagogical introduction (2010).

[23] J. Stokes, J. Izaac, N. Killoran, and G. Carleo, Quantum natural gradient, Quantum **4**, 269 (2020).

[24] J. Gacon, C. Zoufal, G. Carleo, and S. Woerner, Si-multaneous perturbation stochastic approximation of the quantum fisher information, Quantum **5**, 567 (2021).

[25] A. Mari, T. R. Bromley, and N. Killoran, Estimating the gradient and higher-order derivatives on quantum hardware, Phys. Rev. A **103**, 012405 (2021).

[26] T. Haug and M. S. Kim, Optimal training of variational quantum algorithms without barren plateaus (2021), arXiv:2104.14543 [quant-ph].